

PNAS

www.pnas.org

Supplementary Information for

FOXM1 drives HPV+ HNSCC sensitivity to WEE1 inhibition

Ahmed Diab^{1,2}, Hakan Gem^{1,3}, Jherek Swanger¹, Hee Yeon Kim¹, Kaleb Smith¹, Grace Zou¹,
Sharat Raju⁴, Michael Kao⁴, Matthew Fitzgibbon⁵, Keith R. Loeb⁶, Cristina P. Rodriguez⁷,
Eduardo Méndez^{1,4,†}, Denise A. Galloway², Julia M. Sidorova⁶ and Bruce E. Clurman^{1,2,*}

Bruce E. Clurman, M.D., Ph.D
bclurman@fredhutch.org

This PDF file includes:

- Figures S1 to S5
- Legends for Movies S1 to S2
- Legends for Datasets S1 to S5
- Supplemental Experimental Procedures
- SI References

Other supplementary materials for this manuscript include the following:

- Movies S1 to S2
- Datasets S1 to S5

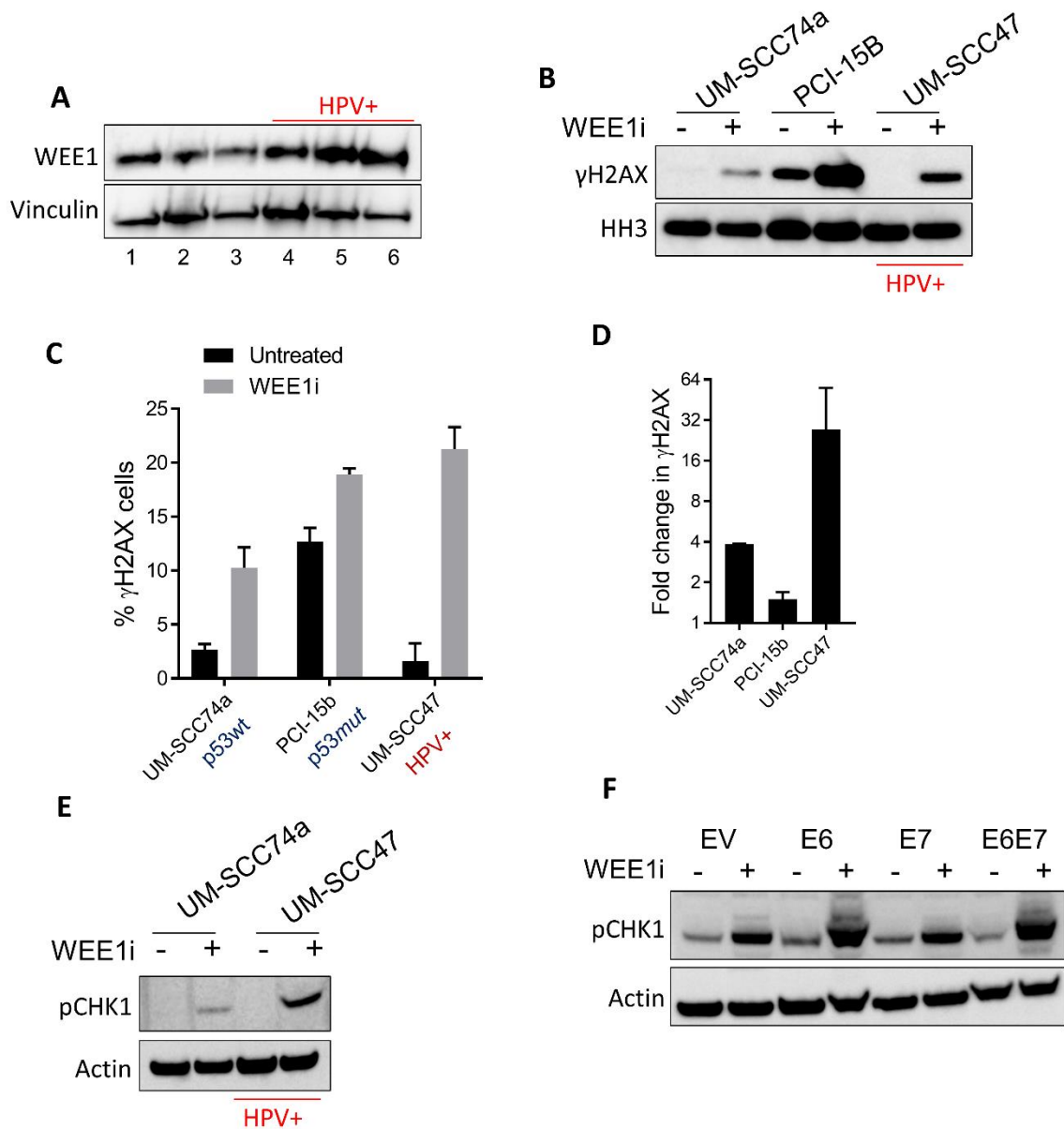


Figure S1: A. Western blots show WEE1 levels in the HPV-negative UM-SCC1 (1), PCI-15b (2), UM-SCC74a (3) cells and the HPV+ UM-SCC47 (4), UPCI-SCC90 (5), UPCI-SCC152 (6) cells. B. Western blots of γ H2AX in the indicated cell lines \pm WEE1i. HPV status is indicated. C. FACS analysis of γ H2AX in the indicated cell lines \pm WEE1i. HPV and p53 mutation status is indicated. Fold change in γ H2AX of FACS data shown in C. E. Western blots of pCHK1 in the indicated cell lines \pm WEE1i. F. Western blots of pCHK1 in EV, E6, E7 and E6E7 UM-SCC74a cells \pm WEE1i.

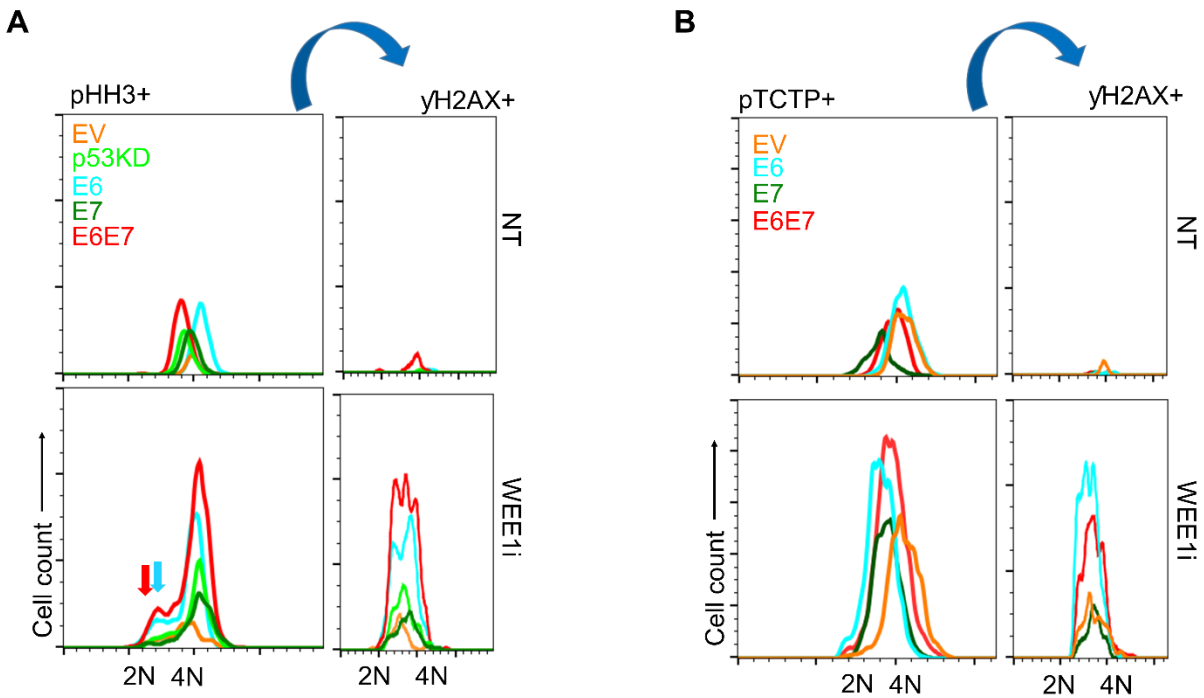


Figure S2: Premature mitosis following WEE1 inhibition is mediated by E6/E7. UM-SCC74a cells treated \pm WEE1i were analyzed by FACS. A. (Left) Histograms of cell-cycle distributions of pHH3+ cells. Only pHH3+ cells are shown. Arrows indicate enrichment of <4N pHH3+ cells among WEE1i-treated E6 and E6/E7 cells. (Right) pHH3+ cells were gated for yH2AX. B. Increased pTCTP (PLK1 substrate) staining in WEE1i-treated E6 and E6/E7 cells (left). pTCTP+ E6 and E6/E7 cells have higher yH2AX (right), indicative of increased DNA damage.

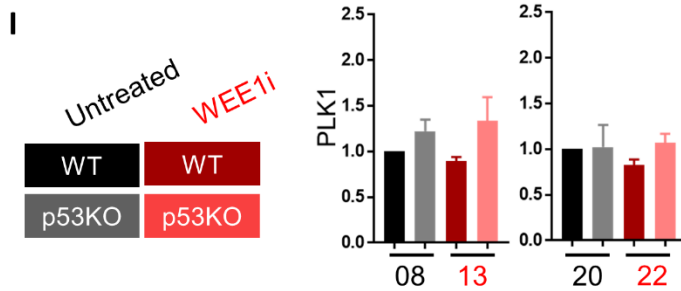
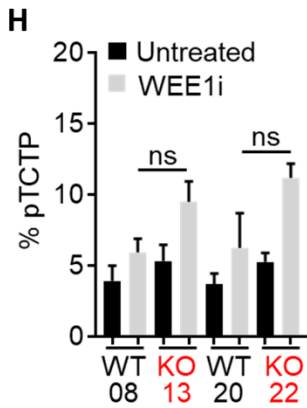
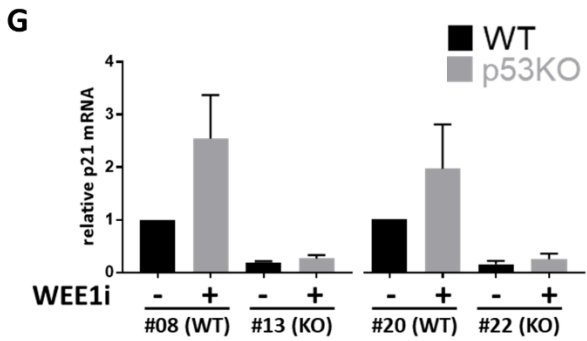
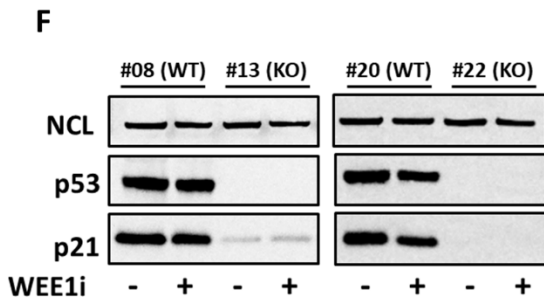
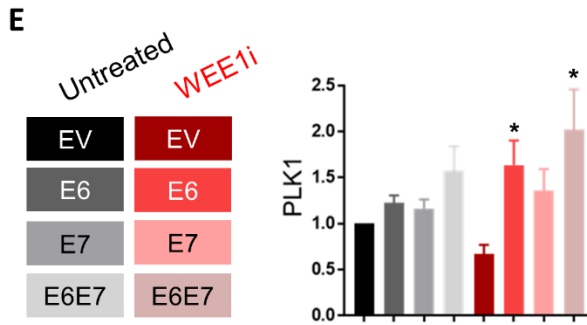
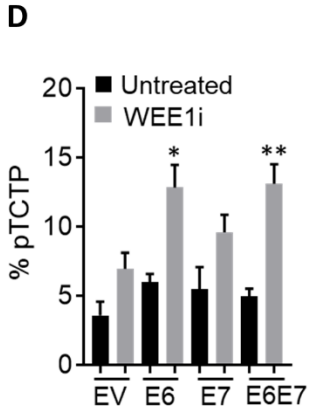
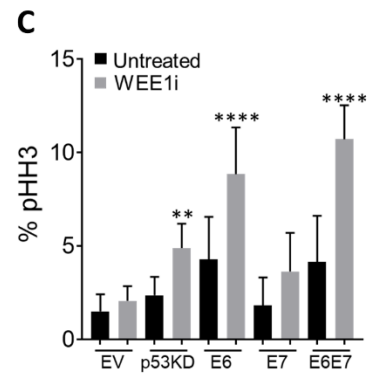
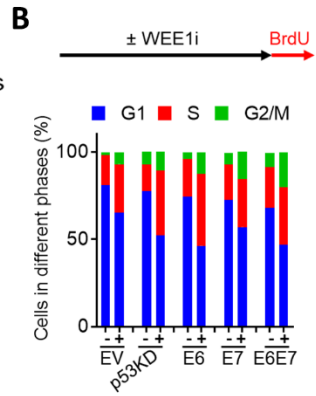
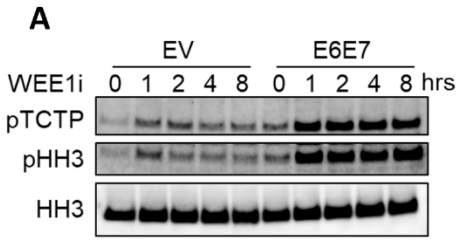


Figure S3: WEE1 inhibition increases the mitotic fraction and PLK1 activity in an E6/E7 dependent manner. A. Western blots of mitotic markers pHH3 and pTCTP (PLK1 substrate) in asynchronous EV and E6/E7 UM-SCC74a cells treated with WEE1i as indicated. B. Cell cycle analysis by FACS in EV, p53KD, E6, E7 and E6/E7 UM-SCC74a cells treated \pm WEE1i followed by BrdU labeling for 30 minutes prior to fixation. C. FACS analysis of pHH3 in EV, p53KD, E6, E7 and E6/E7 cells \pm WEE1i, **= $P \leq 0.01$, ****= $P \leq 0.0001$ ($n > 4$). D. Percentages of pTCTP+ cells from FACS analysis of EV, E6, E7 and E6/E7 cells \pm WEE1i as a measure of PLK1 activity, *= $P \leq 0.05$ ($n = 3$). E. Quantitative RT-PCR analysis of *PLK1* expression in EV, E6, E7 and E6/E7 UM-SCC74a cells treated \pm WEE1i. F. Western blots to confirm deletion of TP53 in UM-SCC74a cells by a CRISPR/Cas9 system. G. Functional suppression of p21Cip1 in p53-/- cells confirmed by quantitative RT-PCR analysis for *CDKN1A*. H. pTCTP staining in p53 +/+ and p53-/- UM-SCC74a clones \pm WEE1i using FACS as in D. Apparent differences do not achieve statistical significance. I. Quantitative RT-PCR analysis of *PLK1* expression in p53 +/+ and p53-/- UM-SCC74a cells treated \pm WEE1i.

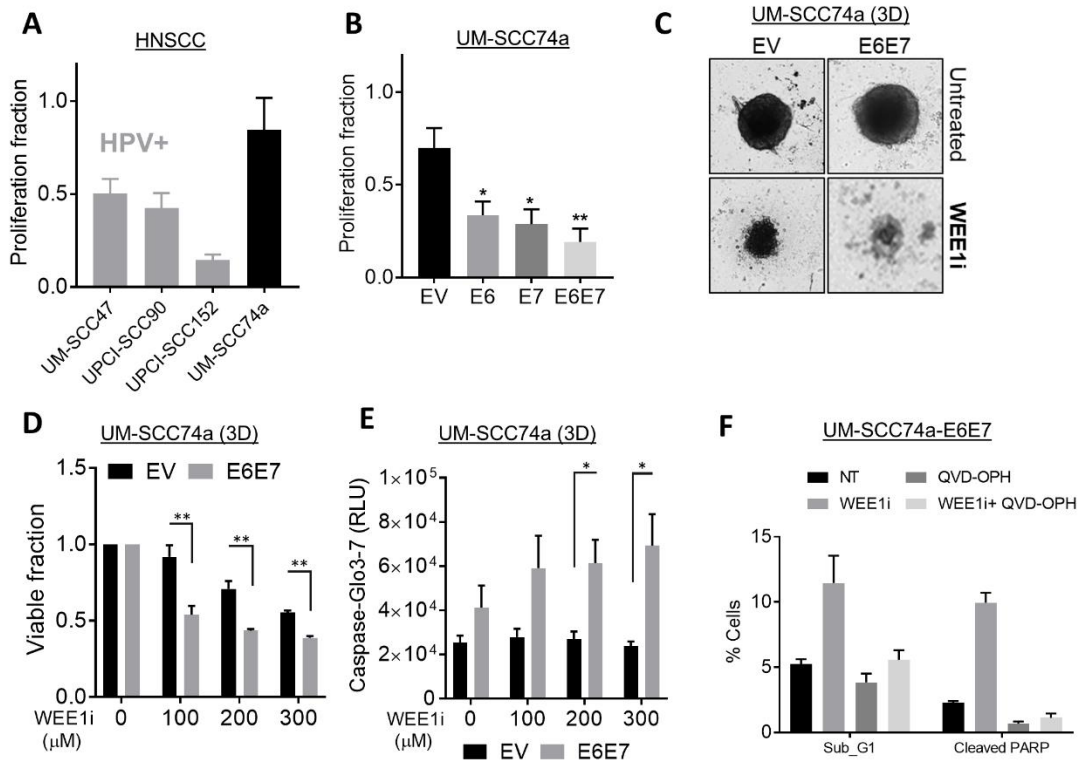
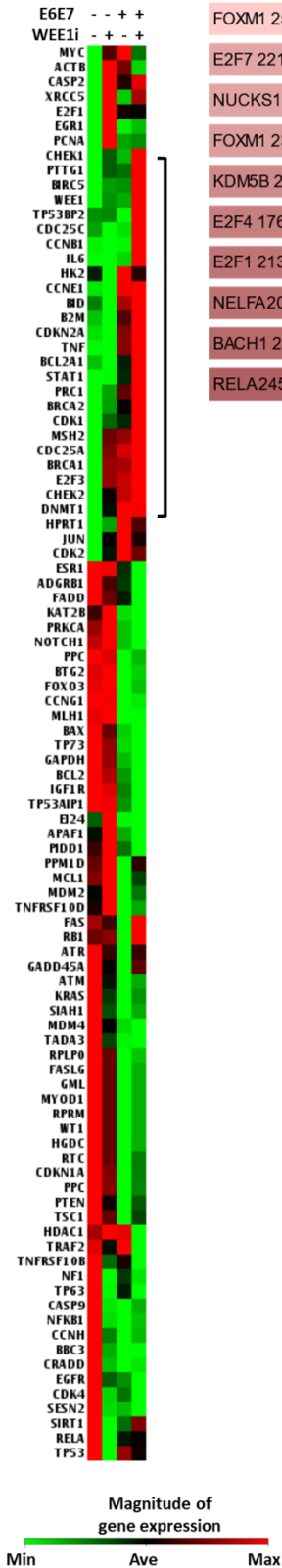
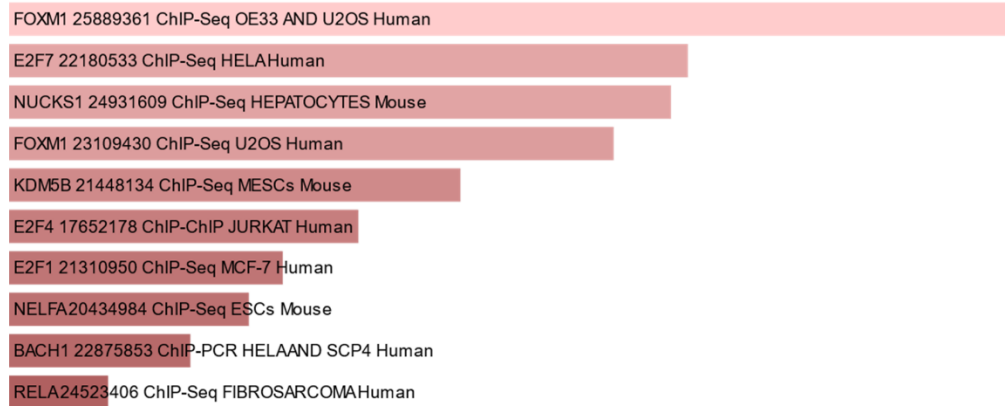


Figure S4: WEE1i induces growth suppression and apoptosis in HPV+ cells. A. Drug washout experiments show HPV-specific sensitivity to WEE1i in HNSCC cells. Quantification of change in proliferation in WEE1i-treated cells relative to mock-treated ($n > 5$). B. Quantification of change in proliferation in WEE1i-treated EV, E6, E7 or E6/E7 UM-SCC74a cells as in A ($n > 3$, $* = P \leq 0.05$, $** = P \leq 0.01$). C. 3D spheroid cultures of EV vs. E6/E7 UM-SCC74a cells treated \pm WEE1i for 6 days. D. Cell viability in 3D cultures was measured using CellTiter-Glo[®] 3D (Promega) 72 hours post-treatment. 3D spheroid cultures of EV vs. E6/E7 UM-SCC74a cells treated with WEE1i as indicated. E. Apoptosis measured using Caspase-Glo[®] 3/7 (Promega) in 3D spheroid cultures of EV vs. E6/E7 UM-SCC74a cells \pm WEE1i as indicated for 24 hours post-treatment. F. A quantitation of sub-G1 cells and cleaved PARP by FACS to measure apoptosis in UM-SCC74a-E6/E7 cells \pm WEE1i. Treatment with QVD-OPH, a pan-caspase inhibitor, rescues WEE1i-induced apoptosis.

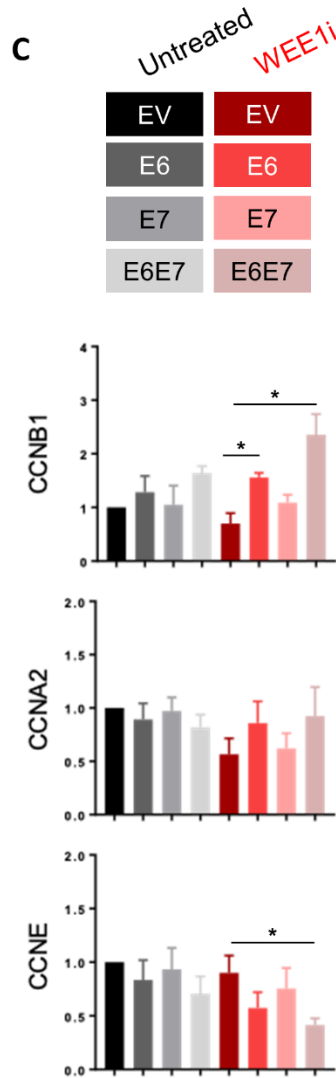
A



B



C



D

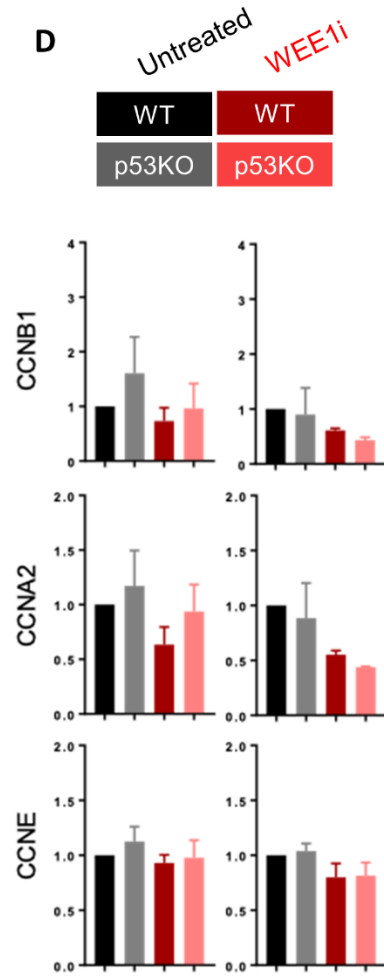


Figure S5: Genomic analysis reveals activation of a FOXM1-target gene network in

WEE1i-treated E6/E7 cells. A. A heat map of the p53 Signaling Pathway RT2 Profiler PCR array analysis of OKF4-hTERT and OKF4-E6/E7 cells treated with \pm WEE1i for 24 hours. B.

Transcription factor motif analysis via Enrichr (amp.pharm.mssm.edu/Enrichr/) using the 25 genes from A that were specifically enriched in WEE1i-treated OKF4-E6/E7 cells. The length of the bar represents the significance of that specific gene-set or term. In addition, the brighter the color, the more significant that term is. FOXM1 is the top hit (p-value 5.186e-9). C. Quantitative RT-PCR analysis of *CCNB1*, *CCNA* and *CCNE* expression in WEE1i-treated EV, E6, E7 and E6/E7 UM-SCC74a cells \pm WEE1i. D. Quantitative RT-PCR analysis of *CCNB1*, *CCNA* and *CCNE* in p53+/+ and p53-/- UM-SCC74a cells \pm WEE1i.

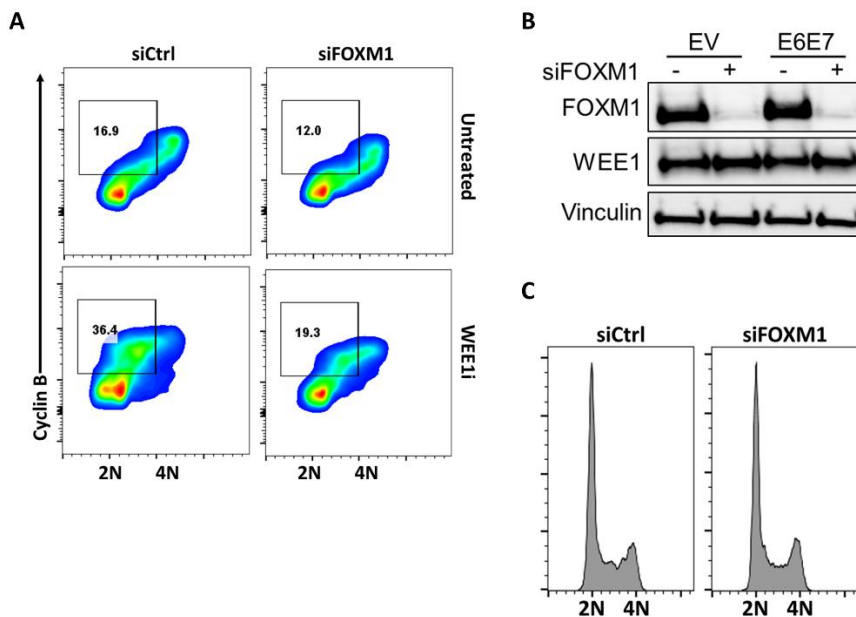


Figure S6: Depletion of FOXM1 in UM-SCC74a E6/E7 cells. A. Representative FACS

analysis of cyclin B in E6/E7 cells \pm WEE1i \pm FOXM1 depletion, gating for interphase cyclin B.

B. Western blots show FOXM1 and WEE1 levels after FOXM1 depletion in EV and E6/E7 UM-SCC74a cells. C. Cell cycle analysis by FACS in control and FOXM1-depleted E6/E7 UM-

SCC74a cells.

Legends for Movies

Movie S1. Live cell imaging of empty vector control UM-SCC74a cells expressing the CDK reporter mVenus-DNA helicase B (DHB). Cells were imaged in full growth media every 12 minutes. After 8 hours of imaging, cells were treated with WEE1i for the next 22 hours of imaging. Cells were then washed and allowed to grow in fresh media without the drug for additional 22 hours of imaging. A representative cell is circled for emphasis.

Movie S2. Live cell imaging of UM-SCC74a-E6E7 cells expressing the CDK reporter mVenus-DNA helicase B (DHB) and treated as in Movie S1.

Legends for Datasets

Dataset S1. List of genes over-expressed in WEE1i-treated E6/E7 keratinocytes.

Dataset S2. List of TF motifs identified using the 25-gene signature from Table S1 using Enrichr.

Dataset S3. Gene set enrichment analysis using fgsea.

Dataset S4. List of antibodies.

Dataset S5. List of oligonucleotides.

Supplemental Experimental Procedures

CRISPR/Cas9 gene knockout of TP53: UM-SCC74a cells were co-transduced with pLenti-Cas9 and sgTP53_3. Transduced cells were selected with puromycin (0.75 µg/mL) and blasticidine (5 µg/mL) for 5 days, then seeded into 96-well plates to yield single cell colonies, which were further expanded and tested for p53 status by immunoblotting. Genomic DNA extracted from selected clones was PCR-amplified with primers encompassing the gRNA target site and sequenced. Clones with protein-truncating INDEL or frameshift mutations in both alleles of the

TP53 gene were used in the subsequent experiments. Some clones with immunoblot- and sequencing-verified wild type *TP53* were used as isogenic wild type controls.

Immunoblotting: Cleared lysates were prepared in NP-40 lysis buffer [50 mM Tris at pH 7.6, 150 mM NaCl, and 0.5% NP-40] supplemented with protease and phosphatase inhibitors. Lysates were normalized via Bradford assay and denatured in Bolt LDS Sample Buffer (Invitrogen) for 10 minutes at 95°C. Alternatively, trypsinized cells were washed in PBS and resuspended directly in 1X Bolt LDS Sample Buffer and denatured for 30 minutes at 95°C to obtain whole cell lysates. Lysates were separated by gel electrophoresis using the Bolt 4-12% Bis-Tris Plus system (Invitrogen). Proteins were transferred to polyvinylidene difluoride (PVDF) membranes via semi-dry transfer, stained with Ponceau Red, and blocked in 5% milk/TBST for at least 1 hour at room temperature. PVDF membranes were incubated in the appropriate primary antibody on a shaker at 4°C overnight. Membranes were subsequently washed with TBST and incubated in secondary antibody (HRP-anti mouse/rabbit IgG, 1:10,000; Cell Signaling Technologies) on a shaker for at least 1 hour at room temperature. Proteins were visualized in a ChemiDoc Touch Imaging System (Bio-Rad) using SuperSignal West Pico PLUS Chemiluminescent Substrate (Thermo Scientific).

Immunoprecipitation and in vitro kinase assay: Cells were lysed directly in their plates on ice using NP-40 lysis buffer [50 mM Tris at pH 7.6, 150 mM NaCl, and 0.5% NP-40] supplemented with protease and phosphatase inhibitors, sonicated for 11 seconds, and centrifuged at 14,000 x *g* for 8 minutes. To pull down our protein of interest, 50 µg of whole cell lysate was incubated with the appropriate primary antibody while rotating in 4°C, followed by a 45-minute incubation with protein A agarose beads. Samples were centrifuged at 10,000 x *g* for 10 seconds, aspirated, and washed three times with lysis buffer. For direct immunoblotting, immunoprecipitated proteins were separated by gel electrophoresis and visualized as described above. Kinase assays were performed as per standard protocol (1).

Flow cytometry: When required, cells were pulse labeled in culture with 10 μ M BrdU for 30 minutes. All cells to be analyzed by FACS were fixed in 2% paraformaldehyde (PFA) for 20 minutes at room temperature, washed once with PBS, resuspended in ice-cold methanol, and allowed to sit overnight at -20°C prior to further processing. Cells were then washed twice with 1 mL BD Perm/Wash Buffer (BD Biosciences), blocked in PBS containing 3%BSA/3%NGS for at least 30 minutes at room temperature, washed once more with 1 mL BD Perm/Wash Buffer, and incubated with the appropriate primary antibodies overnight at 4°C. The next day, cells were washed, incubated in secondary antibody for at least one hour and in DAPI for at least 15 minutes, washed again, and resuspended in Stain Buffer (FBS – BD Biosciences). Samples were run on a BD FACSCelesta, FACSsymphony, or LSRFortessa X-50, visualized with FACS Express software (DeNovo), and analyzed using FlowJo software v10.6.1.

Immunofluorescence and quantitative image-based cytometry (QIBC): To visualize cells by immunofluorescence, cells were initially seeded on coverslips in 12-well plates with 7.5×10^4 cells per well. Following drug treatments, cells were fixed in 2% paraformaldehyde (PFA) for 20 minutes at room temperature, washed once with PBS, and permeabilized with 0.5% Triton-X in PBS for 10 minutes at room temperature. Coverslips were incubated overnight at 4°C with the appropriate primary antibodies diluted 1:100, face-down on parafilm. The next day, coverslips were washed three times with PBS for 5 minutes and incubated in secondary antibody at 1:1000 while shaking for 1 hour at room temperature. Coverslips were washed again with PBS and mounted onto imaging plates with ProLong™ Glass Antifade Mountant with NucBlue™ Stain (Thermo Scientific). QIBC was performed as described previously (2). Cells were considered γ H2AX-positive if their mean γ H2AX signal was $> \frac{1}{2}$ MAX of the population distribution, and the percentage of these cells was calculated for each sample, expressed as fold enrichment over the control at time point 0 hours recovery in each experiment, and averaged.

Comet assays: DNA strand breaks were measured using the CometAssay Kit in alkaline conditions following the manufacturer's protocol (Trevigen). Tail moments, defined as the product of tail length and fraction of total DNA in the tail, were determined using ImageJ software (NIH) with the Open Comet plugin for at least 500 nuclei in each experimental condition. At least 2 independent experiments were scored and pooled.

Cell proliferation assays: Clonogenic assays were performed by first treating cells with 300 nmol/L WEE1i for 17 hours, washing out the drug with PBS, and reseeding each line at 1,000 cells per well in 6-well plates. Cells were allowed to grow undisturbed for 2 weeks until the untreated control cells were nearing confluency. Cells were fixed using a glacial acetic acid and methanol solution at a 1:7 ratio, incubated at room temperature for at least two minutes, washed, and stained with 0.05% crystal violet for at least 20 minutes at room temperature. After washing out the crystal violet solution, plates were allowed to dry overnight, scanned into digital format, and assessed visually for differences in proliferation. Quantification of proliferation fraction was done in ImageJ (NIH). All treatments were performed in duplicate and each experiment was repeated at least three times.

3D Cell viability and Apoptosis Assays: 2×10^3 UM-SCC74a cells were seeded in 96-well ultra-low attachment plates (Corning) and were allowed to form spheroids for 48 hours. Spheroids were treated with increasing concentrations of WEE1i for 24 or 96 hours to assess apoptosis or viability, respectively. 3D CellTiter-Glo (Promega) was used to assess cell viability and Caspase_Glo_3/7 (Promega) was used to assess apoptosis according to the manufacturer's protocols.

Reverse transcription and quantitative real-time PCR (RT-PCR & qPCR): Total RNA was isolated from cells using the RNeasy Mini Kit (Qiagen) according to the manufacturer's protocol and quantified using the NanoDrop One Microvolume UV-Vis Spectrophotometer (Thermo Scientific). One μ g of total RNA was reverse transcribed into cDNA using the iScript Reverse

Transcription Supermix for RT-qPCR (Bio-Rad) according to the manufacturer's protocol. The resulting cDNA was subjected to quantitative real-time PCR using the Platinum SYBR Green qPCR SuperMix-UDG with Rox (Invitrogen) in the ABI QuantStudio5 Real Time PCR System (Thermo Scientific). Each sample was represented in triplicate within 96-well plates. *mRNA* expression levels were normalized to the housekeeping gene *Actin*. The $2^{-\Delta\Delta CT}$ method was used to calculate differential mRNA expression between experimental and control samples.

Analysis of TCGA HNSC RNA-seq data: We downloaded all 500 TCGA HNSC primary tumor RNA-seq data sets from the GDC data portal (<https://gdc.cancer.gov/>) along with a table of clinical covariates for each. Raw RNA-seq counts were processed with edgeR version 3.28.1(3, 4). Raw counts were loaded along with Gencode Human Release v22 GTF file to map Ensembl gene identifiers to approved gene symbols, gene lengths, and other annotations. Data were filtered to remove genes with low overall abundance. To adjust for composition biases, samples were normalized with the TMM method. Tests for differentially expressed genes between HPV+ and HPV- samples were performed with the edgeR quasi-likelihood method (glmQLFit & glmQLFTest). RNA-seq data for representative FOXM1 target genes was visualized as box-and-whisker plots comparing abundances between HPV+ (red) and HPV- (blue) for each gene tested.

Gene set enrichment analysis: To assess whether FOXM1 targets are enriched in HPV+ vs. HPV- we created a gene set from targets described in Table S8 of Fischer 2016 (5) and applied the gene set test method, fgsea (version 1.12.0). Genes that did not survive abundance filtering, including twelve histone genes and one read-through (MsSH5-SAPCD1) that would be difficult to distinguish with annotations used by the TCGA, were excluded. Of the original 282 genes in the set we retained 270 FOXM1 targets for testing. Of the 2159 gene sets tested, fgsea identified 171, including FISCHER_FOXM1, as significantly enriched at FDR < 0.01.

SI References:

1. B. T. Hughes, J. Sidorova, J. Swanger, R. J. Monnat, B. E. Clurman, Essential role for Cdk2 inhibitory phosphorylation during replication stress revealed by a human Cdk2 knockin mutation. *Proc. Natl. Acad. Sci.* **110**, 8954 LP – 8959 (2013).
2. A. Diab, *et al.*, Multiple Defects Sensitize p53-Deficient Head and Neck Cancer Cells to the WEE1 Kinase Inhibition. *Mol. Cancer Res.* (2019).
3. M. D. Robinson, D. J. McCarthy, G. K. Smyth, edgeR: a Bioconductor package for differential expression analysis of digital gene expression data. *Bioinformatics* **26**, 139–140 (2010).
4. D. J. McCarthy, Y. Chen, G. K. Smyth, Differential expression analysis of multifactor RNA-Seq experiments with respect to biological variation. *Nucleic Acids Res.* **40**, 4288–4297 (2012).
5. M. Fischer, P. Grossmann, M. Padi, J. A. DeCaprio, Integration of TP53, DREAM, MMB-FOXM1 and RB-E2F target gene analyses identifies cell cycle gene regulatory networks. *Nucleic Acids Res.* **44**, 6070–6086 (2016).